Specific formation of (M-H)⁻ ions from OH-group-containing molecules

Yu.V. Vasil'ev[a,b,*], M.V. Muftakhov[b], G.M. Tuimedov[b], R.V. Khatymov[b], R.R. Abzalimov[b], V.A. Mazunov[b], T. Drewello[a]

[a]*Department of Chemistry, University of Warwick, Coventry CV4 7AL, England*
[b]*Institute of Physics of Molecules and Crystals, Ufa Research Centre of Russian Academy of Science, Ufa 450000, Russia*

Abstract

The formation of (M-H)⁻ ions from OH-containing benzene derivatives, covering azobenzenes and phenols, has been investigated by resonant electron-capture mass spectrometry. A vibrational fine structure in the effective ion yield curves, at threshold energies for the formation of these ions through OH-bond cleavage, has been observed. This vibrational progression has been assigned to the ν(OH) stretching mode. It has been supposed that the formation of these ions occurs by a predissociation of the vibrationally excited ground state of the parent anion. (Int J Mass Spectrom 205 (2001) 119–135) © 2001 Elsevier Science B.V.

1. Introduction

The formation and decomposition of positive ions in mass spectrometry are usually well described by a variety of statistical theories, the most common of which are the RRKM and the quasi-equilibrium theory (QET). At the heart of these methods are two assumptions, ergodity and the transition state approximation [1,2]. In terms of a statistical approach, a unimolecular reaction is considered as a flux in phase space through a critical surface. If this phase space is uniformly sampled, the rate constant of the reaction is a smooth, monotonically increasing function of the

internal energy. The validity of the last assumption, especially in connection with the development of monoenergetic sources for molecular excitation, has been the subject of many investigations. It has been established that unlike fast bimolecular reactions and apart from a few exceptional cases, the unimolecular reactions are in fairly good agreement with the statistical models. The question that frequently arises concerns a complicity of the phase space sampling, but even in these cases it was shown that the rate constant is rather insensitive to incomplete intramolecular vibrational energy relaxation and nonuniform sampling of phase space [2,3].

Statistical aspects of negative ions have also been discussed in the literature [4] and it is necessary to stress some specifics of negative ions, which are relevant in this context. Representation of the nega-

---

* Corresponding author. E-mail: y.vasilev@warwick.ac.uk
Dedicated to Professor Alex Stamatovič on the occasion of his sixtieth birthday.

tive ions only as a species with the opposite charge to positive ions is a simplification of the real nature of negative ions. Indeed, collisions of low-energy electrons with molecules resulting in the formation of molecular negative ions have essentially resonant character. Therefore, it is appropriate in this case to speak about mode-selective physics and chemistry, at least in terms of the electronic states. The second important factor of relevance to the statistical model of the negative molecular ions is their metastability with respect to electron autodetachment processes. (A very similar process occurring on the same time scale was recently discovered for positive ions of large cluster molecules and fullerenes and was named delayed ionisation [5].) Electron autodetachment for negative ions is an important obstacle for the total, or very frequently even for the partial, randomization of the internal energy among the various molecular vibrational modes. For instance, even for fullerenes, with their huge density of states [6], the statistical models do not adequately describe the processes of electron autodetachment [7–10], contrary to positive ions, where the situation is much clearer [6]. Probably only half of the total number of vibrations are active in the electron autodetachment processes in fullerene anions with an internal energy of approximately 15 eV [11]. Thus, fast dissociation of negative ions is a rather common process. Observations such as the direct isotope effect [12] associated with dissociative electron capture and the unstructured, bell-shaped effective yield curves of fragment negative ions are strong indications for these fast dissociation processes. Hence, it is not surprising that formation and dissociation of negative ions follow different selection rules [13–18].

However, there also exists ample evidence for slow negative ion decay. Proof for these slow dissociations results from inverse and small direct isotope effects (or from their absence) [12,19], as well as from the vibrational structure in the negative ion yield curves (see [20] and references cited therein), metastable peaks in the negative ion mass spectrum, and the occurrence of hidden rearrangements [21]. The ability to undergo fragmentations on a longer time scale is particularly important when exploring the capture of low-energy electrons, where the lifetimes of the resonant states of the parent negative ions are supposed to be longer. The selection rules for these cases are totally different from what is valid for the fast dissociation processes, and application of the selection rules in the simplest form, that is, based only on the symmetry of the electronic part of the wave function, is hardly justified.

The present investigation is concerned with the formation of (M-H)$^-$ ions from selected OH-containing precursors applying resonant electron capture mass spectrometry. We have previously reported [22] on the observation of (M-H)$^-$ ions from p-OH-azobenzene (AzB) that were generated by cleavage of the OH bond in the low-energy range. Interestingly, the effective yield curves of these ions contained a vibrational fine structure showing a spacing between peaks close to the ν(OH) stretching mode. Less pronounced, but nevertheless very similar, vibrational progression in the curves of analogues (M-H)$^-$ were later observed in the case of carbonyl compounds [23] and acridanoneacetic acid [24]. The observation of such a vibrational progression contradicts recent assumptions concerning the (M-H)$^-$ ion formation, in which a fast dissociation from an out-of-plane conformational arrangement of the hydroxy-hydrogen atom is of central importance [25,26]. In these investigations, the low-energy formation of (M-H)$^-$ ions from OH- and NH$_2$-containing derivatives of benzothiadiazole and anthraquinone was assigned as a symmetry forbidden process. A molecular conformation with an out-of-plane position of the hydroxy H-atom, for which this process is not forbidden, was assumed responsible for the (M-H)$^-$ ion formation. The restricted rotation of the OH group and the OCH$_3$ group in pentafluorophenol and pentafluoroanisole was also previously noted [27]. It was stressed [25] that at room temperature ~4% of the molecules are in this out-of-plane conformation, seemingly in accordance with the observed relative intensity of 2% and 11% for these ions. However, there are several points of concern that cast doubts on the validity of those assumptions. For instance, there

exists no basis for a quantitative comparison involving the abundances of the molecular anions generated at zero energy, as their formation follows an entirely different process, that is, nondissociative electron capture. Also, it is well known that the cross section for thermal energy attachment, if there are no restrictions, is very large. Hence, it would be more appropriate to make a comparison with the abundances of other fragment ions originating from the same resonant state or, at least, from the neighbouring resonances, if other dissociation channels are closed in this resonance for some reason. Moreover, according to calculations [25], the potential energy surface, as a function of the torsion angle, does not possess any minima for out-of-plane conformations. And finally, although the molecules with NH_2-substitutions have no symmetry restrictions for the formation of $(M\text{-}H)^-$ ions by cleavage of the N-H bond, they were found [25] with lower relative intensity than $(M\text{-}H)^-$ ions from compounds containing an OH-group.

In the following article the $(M\text{-}H)^-$ ion formation at low energies is investigated in detail applying resonant electron capture mass spectrometry. This study covers several aromatic compounds, all of which posses only one OH-group including compounds where hydrogen is only present in the hydroxyl-group. The molecules under investigation were: phenol (1), *p*-nitrophenol (2), *p*-chlorophenol (3), pentachlorophenol (4), *p*-OH-AzB (5), *p*-OH-*p'*-NO$_2$-AzB (6), *p*-OH-*p'*-CH$_3$-AzB (7), *p*-OH-*p'*-OCH$_3$-AzB (8), *p*-NO$_2$-AzB (9), *p*-OCH$_3$-*p'*-OCH$_3$-AzB (10) and trifluoroacetic acid (TFA) (11). Compounds 9 and 10, which do not contain an OH-group, were investigated for comparison.

2. Experimental

Resonant electron capture spectra were studied using a modified single-focusing sector-type mass spectrometer MI 1201. For details of the instrumentation see elsewhere [11]. Briefly, negative ions were formed in the ionization chamber of the mass spectrometer as a result of the interaction of an electron

beam with an effusing molecular beam. The electron beam was of variable energy and was generated by a computer-controlled trochoidal electron monochromator. In operation, the electron energy resolution was $\Delta \varepsilon \approx 70 - 120$ meV Full width at half-maximum (FWHM) at an electron current of $\approx 5 - 50$ nA. In principle, it is possible for this monochromator to operate with a better energy resolution (<20–25 meV); however, in the present investigation, the use of a smaller electron energy spread was impossible because of the low intensity of the ion signals. The molecular beam for the compounds under investigation was obtained by heating a solid probe in the direct inlet system to get sufficient vapor pressure, whereas liquids or gases were driven into the ionization chamber through a capillary. In operation, the pressure measured with an ion gauge outside the ionization chamber was not higher than 10^{-8}–10^{-9} Torr, which corresponds to single-collision conditions, preventing any additional ion–molecule scattering in the ionization chamber. In agreement with these conditions, a linear dependence of the ion signals on the pressure has been observed within this pressure range. For the temperature dependence experiments, the temperature of the inlet system was kept constant in order to prevent variations of the molecular flux during the experiment, while the temperature of the ionization chamber was varied. Before effusing into the ionization chamber, the molecules underwent many collisions with the walls of the special entrance channel ("antiskimmer"), which was held at the same temperature as the ionization chamber. The extracted and focused negative ions were accelerated by 4 kV, mass analyzed, and then detected by an electron multiplier. The obtained data were accumulated by a computer. In the registration of negative ions, the electron energy scale was calibrated using the maximum of the effective yield curves of SF_6^- (≈ 0 eV) and NH_2^- from NH_3 (5.65 eV). Determination of the mean lifetime of the negative ions was achieved as described in [11], and a detailed description of the measurements of the appearance energies of negative ions has been reported elsewhere [23,24].
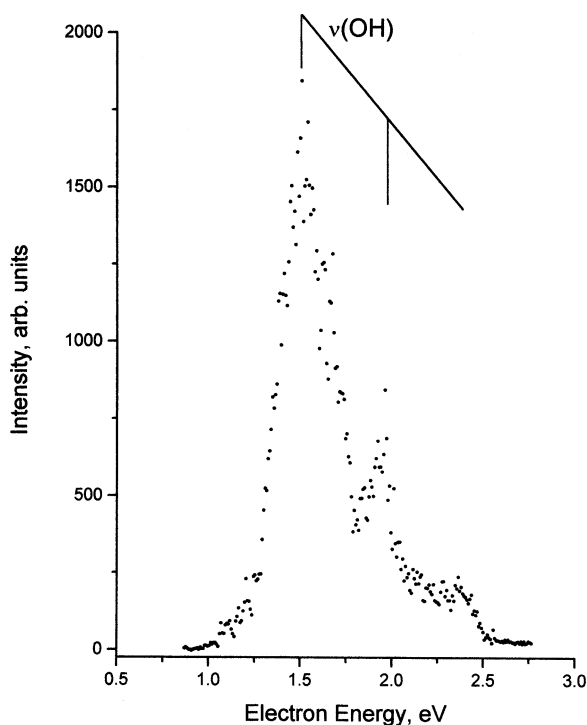
Fig. 1. Effective yield curve of the $C_6H_5O^-$ negative ions from phenol, plotted as a function of electron energy. Bars indicate the vibrational progression of the ν(OH) stretching mode.

Fig. 2. Effective yield curve of the $NO_2C_6H_5O^-$ negative ions from nitrophenol, plotted as a function of electron energy at two temperatures: 170 °C (top) and 345 °C (bottom). Bars indicate the vibrational progression of the ν(OH) stretching mode.

3. Results

3.1. Phenol and its derivatives

Interactions of low-energy electrons with benzene molecules and their derivatives have been comprehensively discussed in the literature (see reviews [28–31]). Staying within the limits of the problem posed, we shall consider here only the formation of (M-H)$^-$ ions from phenols in conjunction with the discussion of some related observations.

Figs. 1–4 show the effective yield curves of (M-H)$^-$ ions from phenol (1), p-nitrophenol (2), p-chlorophenol (3), and pentachlorophenol (4), respectively. Based on simple energetic reasons (see below for details), the registration of these ions in the energy range of 0.5–2.5 eV is definitely associated with OH-bond cleavage, as the analogous process of C-H bond cleavage, resulting in the formation of ions of the same mass, can occur only at energies >3 eV.
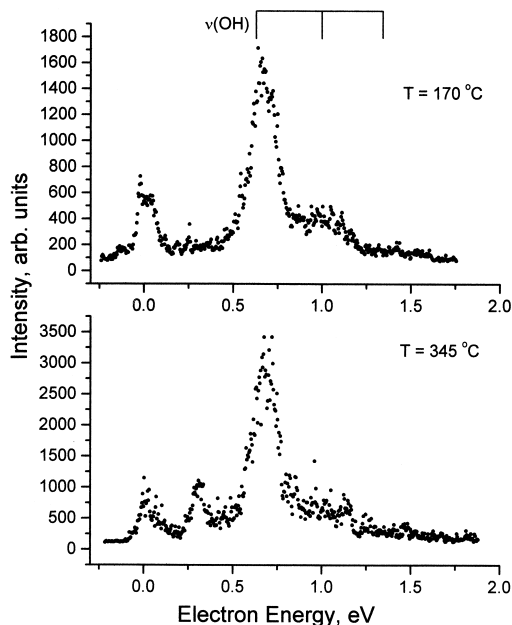
The common feature of the curves in this energy range is the occurrence of a more or less pronounced vibrational progression. Depending on the compound, the spacing between neighbouring peaks in the progression varies from 0.38 to 0.43 eV, which might be attributed to a ν(OH) or a ν(CH) stretch mode. In order to solve this question staying within the same electron energy resolution, we examined compound 4 and TFA (see below). The study of these two compounds is particularly important, as they make up only one type of hydrogen atom and have only one high-frequency mode, which is the ν(OH). In the case of compound 4, there was no prominent vibrational structure observed; instead, we obtained only a broad feature with a washed-out structure at the high-energy end of the most pronounced resonant peak. This observation is probably caused by a dramatic contamination of the ion source with sample vapor resulting in the destruction of the energy distribution of the electron beam. Nevertheless, there is no doubt that this spread-out, unresolved structure has the same
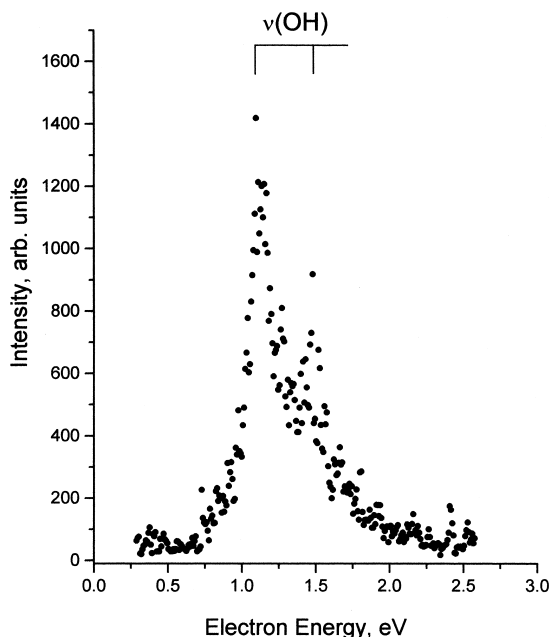
Fig. 3. Effective yield curve of the $ClC_6H_4O^-$ negative ions from *p*-chlorophenol, plotted as a function of electron energy. Bars indicate the vibrational progression of the $\nu(OH)$ stretching mode.

Fig. 4. Effective yield curve of the $C_6Cl_5O^-$ negative ions from pentachlorophenol, plotted as a function of electron energy. The inset shows the expanded energy scale in the range from ~0 to 2 eV. Bars in the inset indicate the vibrational progression of the $\nu(OH)$ stretching mode.

origin associated with the excitation of the $\nu(OH)$ stretching mode. Indeed, we shall indicate below that a much more prominent vibrational fine structure in the effective yield curve of the $(M-H)^-$ ions from TFA gives an unambiguous confirmation for this assignment.

In addition to the vibrational progression with the main peak at 0.65 eV, another resonant peak at zero energy was registered in the yield curve of the $(M-H)^-$ ions derived from nitrophenol 2 (Fig. 2). Experiments on the temperature dependence of the resonant electron capture spectra of 2 showed that one additional resonant peak of $(M-H)^-$ ions was observed at elevated temperatures. Its energy was determined to be less than the energy of the main peak at 0.65 eV, the difference being exactly equal to the vibrational quanta of $\nu(OH)$.

The half-widths of the resonant peaks in the vibrational progression were found to be different for the various target compounds. As an example, the FWHM of the resonant peak at ~1.5 eV from phenol amounts to 0.38 eV (the energy resolution, $\Delta\varepsilon$,
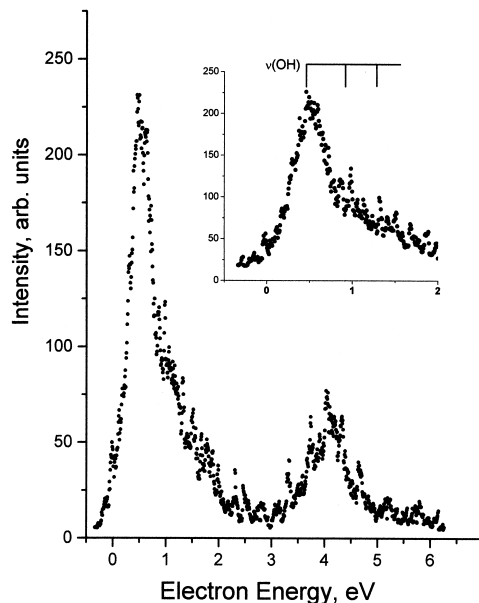
estimated by the parallel recording of the SF_6^- curve, was 120 meV), whereas for nitrophenol, 0.176 eV were found (at the resonant peak 0.65 eV and $\Delta\varepsilon = 100$ meV). Both these measurements were conducted at roughly the same effective temperature of 370 K.

The appearance energy (AE) of $C_6H_5O^-$ ions from phenol, determined as described in [23,24], was established to be 1.29 ± 0.05 eV. This value is slightly lower than the thermochemical threshold (1.497 eV) established from the following equation:

$$AE\ [(C_6H_5O)^-] = \Delta H_f[C_6H_5O] - EA\ [C_6H_5O]$$
$$+ \Delta H_f[H] - \Delta H_f[C_6H_5OH], \quad (1)$$

with the enthalpy of formation $\Delta H_f[C_6H_5O] = 47.7$ kJ mol^{-1}, electron affinity EA $[C_6H_5O] = 2.253 \pm 0.006$ eV, ΔH_f [H] $= 217.8$ kJ mol^{-1} and $\Delta H_f[C_6H_5OH] = -96.4$ kJ mol^{-1}. All these thermochemical data were taken from [32]. It should be noted, however, that the energy of the resonant peak,

~1.5 eV, matches rather well with this thermochemical threshold.

AE [(NO$_2$C$_6$H$_4$O)$^-$] for nitrophenol at the resonant peak of 0.65 eV was determined to be 0.57 ± 0.04 eV. As one can see from Figs. 3 and 4, the AE [(Cl$_x$C$_6$H$_y$O)$^-$] values from compounds 3 ($x = 1$, $y = 4$) and 4 ($x = 5$, $y = 0$) were also lower than that of the analogous ion from 1. There are two main factors probably influencing this value, namely the bond dissociation energy, BDE, of the OH-bond and the electron affinity of the oxy-radical. Considering the BDE's in methane derivatives [32,33], it results that the nitro group may slightly stabilize the bond (by 2–3 kcal mol^{-1}), whereas the influence of halogen atoms is slightly stronger and of a destabilizing nature: BDE [CH$_3$-H] = 105.1 kcal mol^{-1}, BDE [NO$_2$CH$_2$-H] = 107 kcal mol^{-1}, BDE [ClCH$_2$-H] = 100.9 kcal mol^{-1}, BDE [Cl$_2$CH-H] = 99.0 kcal mol^{-1}, and BDE [Cl$_3$C-H] = 95.8 kcal mol^{-1}. Based on this, we can also conjecture that the BDE [H-OC$_6$H$_4$NO$_2$] should be slightly higher compared to that of 1 and, therefore, the experimentally observed decreasing AE [(NO$_2$C$_6$H$_4$O)$^-$] is practically entirely connected with the high electron-affinity value of the oxy-radical. In the case of chlorophenols 3 and 4, we think that both factors (low BDE and higher EA with respect to 1) lead to a decrease of the AE [(Cl$_x$C$_6$H$_y$O)$^-$]. Indeed, we have obtained very similar tendencies from semiempirical calculations (AM1 and PM3 methods, full-energy optimization of geometry) of the enthalpy of formation of phenol derivatives. The theoretical appearance energies of the XC$_6$H$_4$O$^-$ ions deduced on the basis of the calculations in the case of X = H (1) and NO$_2$ (2) were 1.447 eV and 1.284 eV (AM1 and PM3, respectively, for 1), and 0.288 eV and 0.525 eV (AM1 and PM3, respectively, for 2). The agreement between the values of the thermochemical limit for the dissociation reaction under discussion, determined by the three independent methods, was quite good. Thus, keeping in mind the possible differences between the BDE for 1 and 2 (~2–3 kcal mol^{-1}) and based on the difference of the AE [(XC$_6$H$_4$O)$^-$] values, we can now estimate the enhancement of the electron affinity of the oxy-radical from 2, with respect to that of 1, to
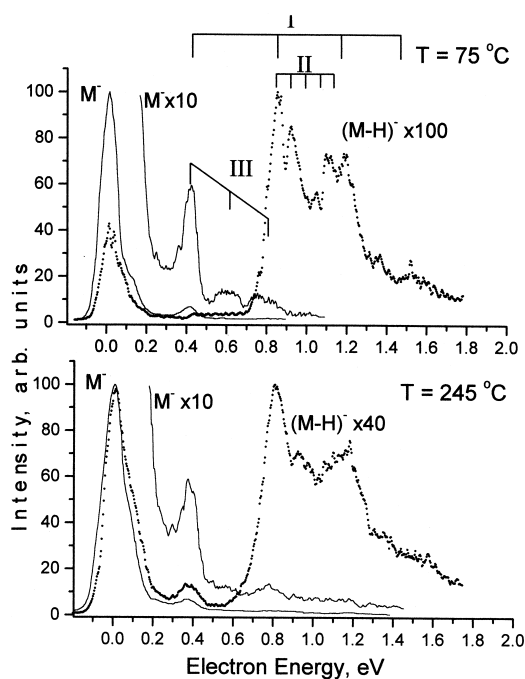

Fig. 5. Effective yield curves of the molecular M$^-$ (solid line) and the fragment C$_6$H$_5$N$_2$C$_6$H$_4$O$^-$ (dots; noted as (M-H)$^-$ in the figure) negative ions from *p*-OH-AzB plotted as functions of the electron energy at the two temperatures of 75 °C (top) and 245 °C (bottom). Bars indicate the different vibrational progressions I, II, and III (see text).

be ~0.8 eV. The analogous phenomenon was reported [34] in the case of furancarbon acid and nitrofurancarbon acid.

3.2. *p*-Hydroxy azobenzene and its derivatives

Resonant electron capture mass spectra of azobenzene and its derivatives, including *p*-hydroxy azobenzene (5), have been previously investigated using moderate energy resolution [35–38]. Resonant electron capture spectra of 5 with better energy resolution were reported in [22]. Fig. 5 depicts the effective yield curves of the molecular negative ions M$^-$ and of the respective (M-H)$^-$ ions. The curves were recorded at different ion source temperatures T, over an energy range of ~0–2 eV. The yield curve of (M-H)$^-$ within a wider energy range is shown in Fig. 6. Azobenzenes are known [35–38] for the formation of long-lived
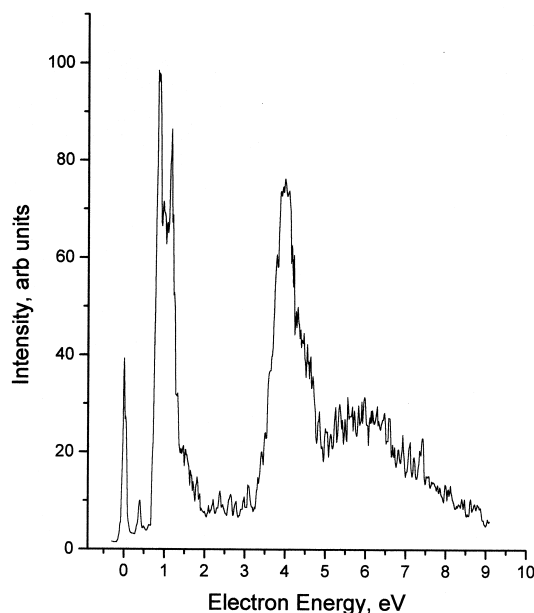
Fig. 6. Effective yield curve of the $C_6H_5N_2C_6H_4O^-$ fragment negative ions from *p*-OH-AzB, plotted as a function of the electron energy in the range from ~0 to 9 eV.

Fig. 7. Mean lifetime curves of the molecular negative ions from *p*-OH-AzB, plotted as a function of the electron energy in the range from ~0 to 1 eV, determined at two temperatures, 75 °C (open circles; the values multiplied by a factor of four are also shown in the energy range 0.4–1 eV) and 180 °C (open triangles). Vertical arrows indicate the position of the resonant vibrational peaks; horizontal dashed lines indicate the mean value of the lifetime within the vibrational peak.

(i.e., mass spectrometrically observable) molecular negative ions in a range of electron energies from zero to 1.5–2 eV. This fact is illustrated for compound 5 in Fig. 7, where the lifetime curves of the molecular ions were plotted against the electron energy at two temperatures.

As one can see from Fig. 5, both molecular and fragment ion yield curves demonstrate vibrational structure, which does not disappear with increasing temperature. The most intriguing fact is that the analogous vibrational progression of the ν(OH) stretch modes (marked as I in Fig. 5) starts in the long-lived molecular negative ion-yield curve and continues in the curve of the (M-H)$^-$ ions. While the absolute position of the first peak in the curve of M$^-$ is displaced on the energy scale, depending on the compound, the spacing between this peak and the next one located on the curve of (M-H)$^-$ ions is constant. Figs. 8–10 demonstrate this fact for the three derivatives of *p*-hydroxy AzB 6, 7, and 8. The lowering of the spacing between the vibrational peaks in the progression testifies to the anharmonicity of these
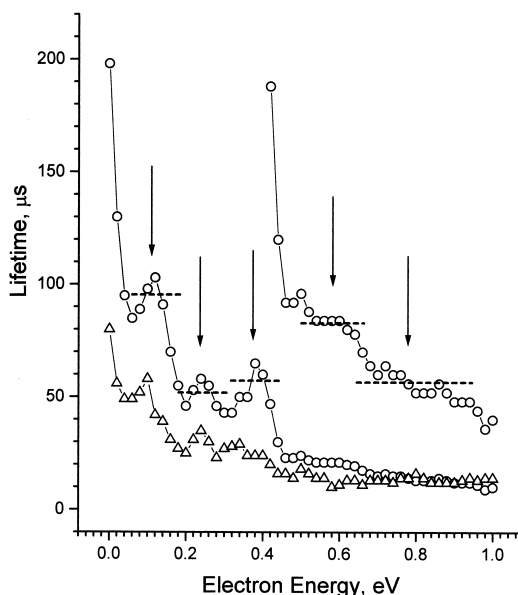
vibrations. It should be noted that the first two vibrational peaks of the progression are especially sharp and narrow, with a FWHM practically equal to that of SF_6^- ($\Delta\varepsilon \approx 70$ meV). This indicates a very long lifetime of the resonant states from which they originate. It is also remarkable that the heights of the two first neighbouring vibrational peaks in the (M-H)$^-$ curve (second and third in the progression) vary for the different compounds. The third peak on the curve (fourth in the progression) is always of low intensity and much broader than previous peaks.

There is another vibrational structure in the curve of the (M-H)$^-$ ions (notation II in Fig. 5), with an average spacing between the vibrational peaks of ~110–115 meV. Considering the present energy resolution and the large number of different vibrations with similar vibrational quanta present in this energy range, the assignment of these vibrations cannot be achieved unambiguously. Actually, several out-of-
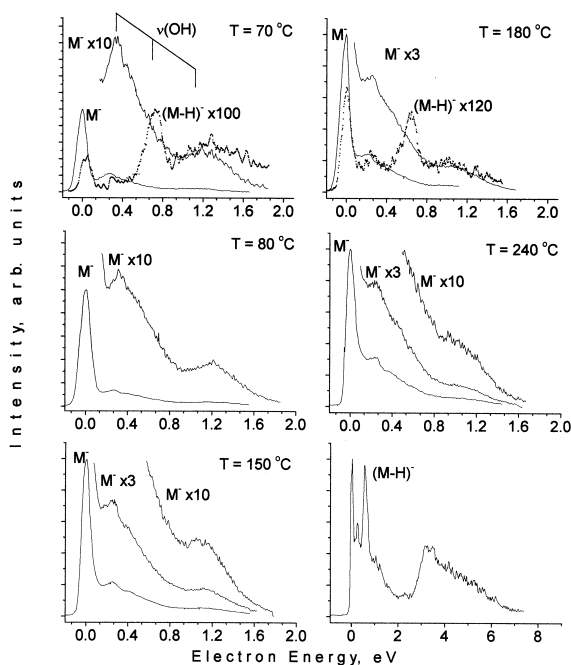
Fig. 8. Effective yield curves of the molecular M^- negative ions (solid lines; recorded at the temperatures: 70°, 80°, 150°, 180°, and 240 °C) and the fragment negative ions $NO_2C_6H_4N_2C_6H_4O^-$ (noted as $(M-H)^-$ in the figure and plotted for two temperatures: 70° and 180 °C) from p-OH-p'-NO_2-AzB as functions of the electron energy. Effective yield curve of $(M-H)^-$ in the energy range from ~0 to 7 eV recorded at 200 °C (right, bottom). Bars indicate the vibrational progression of the $\nu(OH)$ stretching mode.

Fig. 9. Effective yield curves of the molecular M^- negative ions (left) and the fragment negative ions $CH_3C_6H_4N_2C_6H_4O^-$ (right; noted as $(M-H)^-$ in the figure) from p-OH-p'-CH_3-AzB plotted as a function of the electron energy at the temperatures of 60°, 140° and 240 °C.

plane vibrational modes in AzBs have close frequencies in the range 880–980 cm^{-1} [39]. The observed vibrational progression could in principle also be assigned to the C-O stretching mode (~128 meV), especially when taking into account the insufficient energy resolution and the possible change to lower values of vibrational quanta in the anion as opposed to the neutral molecule.

An additional vibrational structure (notation III in Fig. 5) with a spacing ~180–200 meV was observed in the yield curve of M^- that we assign to N=N or C=C stretch modes. Both the progressions II and III are washed out over the curves with increasing temperature. There is also a shoulder on the high-energy side of the thermal resonant peak of M^- (0.1–0.12 eV) in the case of all the compounds under investigation.
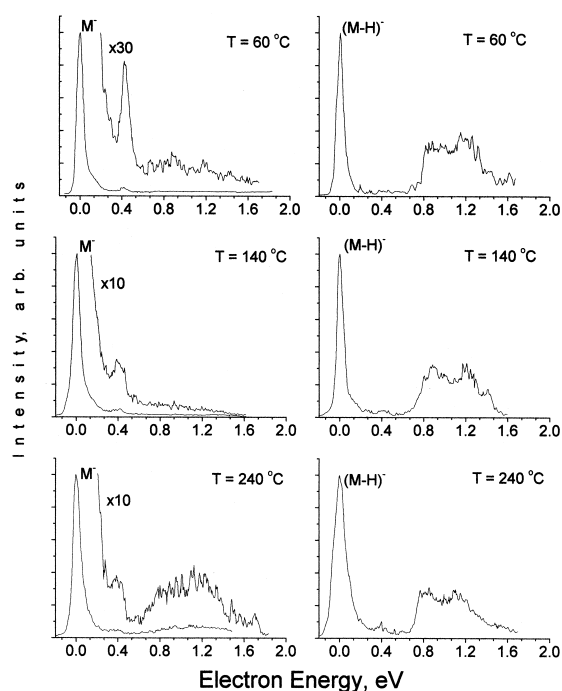
Another common feature is a decreasing mean lifetime, τ, with respect to electron autodetachment at thermal energies with elevated temperatures. Fig. 7 shows this phenomenon for the example of compound 5 at two fixed temperatures. It is also interesting to note that practically all the resonant features of the effective yield curve of M^- are very well reflected in the mean lifetime curves (cf. Figs. 5, 7). This seems to be an indication for the remarkable fact that the magnitude of the M^- lifetime is almost constant within a separate resonant vibrational peak. To the best of our knowledge, such an observation has not been published before. Up to ~0.7 eV, τ decreases in value with the temperature, whereas at higher energies, it is practically unchanged by the temperature variation. Compound 8 showed a very similar energy and temperature dependence of the parent anion lifetime curve. In the case of compound 7, a rather unusual phenomenon of a simultaneous increase of
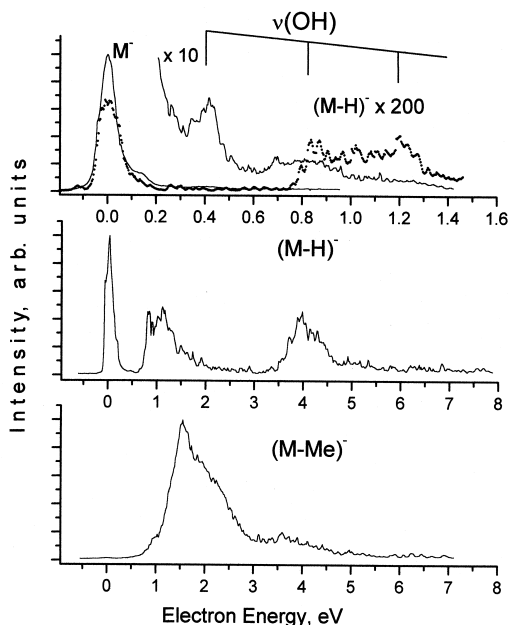
Fig. 10. Effective yield curves of the molecular M⁻ (solid line) and the fragment H₃COC₆H₄N₂C₆H₄O⁻ (dots; noted as (M-H)⁻ in the figure) negative ions from *p*-OH-*p′*-H₃CO-AzB, plotted as functions of the electron energy in the energy range ~0 to 1.5 eV (bottom); bars indicate the vibrational progression of the ν(OH) stretching mode. Effective yield curve of the (M-H)⁻ fragment negative ions in the range from ~0 to 8 eV (middle). Effective yield curve of the (M-H)⁻ fragment negative ions in the energy range from ~0 to 9 eV (bottom).
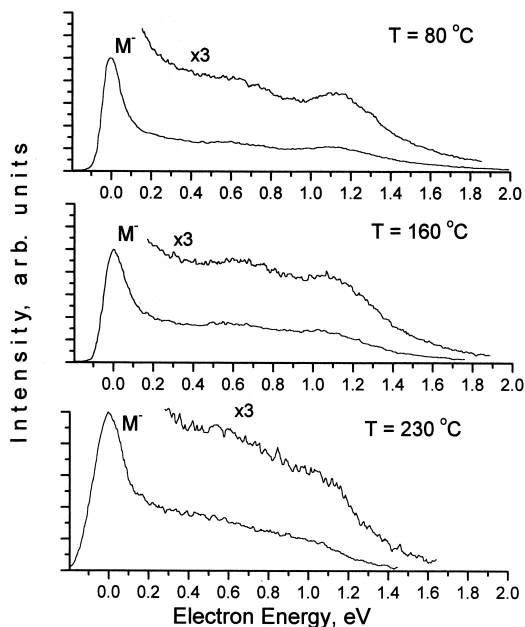

Fig. 11. Effective yield curves of the molecular negative ions from *p*-NO₂-AzB plotted as a function of the electron energy recorded at temperatures of 80°, 160°, and 230 °C.

intensity and mean lifetime of M⁻ in the energy range of 0.9–1.4 eV (Fig. 9) has been established when increasing the temperature.

It is interesting to note that the shape of the effective yield curve of M⁻ from compound 6 (*p*-OH-*p′*-NO2-AzB) represents a simple addition of the M⁻ curves of compound 5 (*p*-OH-AzB) and compound 9 (*p*-NO₂-AzB); (cf. Figs. 5, 8, 11). As mentioned above, the energy at which the vibrational progression of the ν(OH) stretching mode commences is different depending on the compound. For 6 it is shifted to lower energies with respect to 5, and the displacement is especially pronounced. Over the large energy range, the lifetime of M⁻ for this compound is also a mean of the two values of τ of M⁻ from 5 and 9, with a higher value for the latter. As a consequence of this, the lifetime of M⁻ from 6 was increased,

showing intact molecular ions in the energy range of 1–1.2 eV, where no parent ions of 5 could be observed, and while long-lived anions of 9 were clearly present at these energies. All these findings strongly indicate that there is only a very weak interaction of the phenyl rings in 6 through the azo-bridge.

The analysis of the temperature dependence of the M⁻ ion abundance of compound 5 at ≈0 eV and of the corresponding (M-H)⁻ ions at the resonant maxima at 0.85 eV and at higher energies shows a clear enhancement with temperature by factors of five and 20, respectively. Regarding the parent anion abundance we have to take a possible reduction caused by electron autodetachment into account. As mentioned in the section 2, we tried to avoid changes in the flux of the effusive molecular beam. Nevertheless, we cannot completely rule out the possibility of increasing the ion intensity as a result of an uncontrolled flux of the molecules, which is of especial concern at higher temperatures. In any case, the intensities of the resonant peaks in the curve of (M-H)⁻ starting at 0.85 eV and continuing at higher energies showed simul-
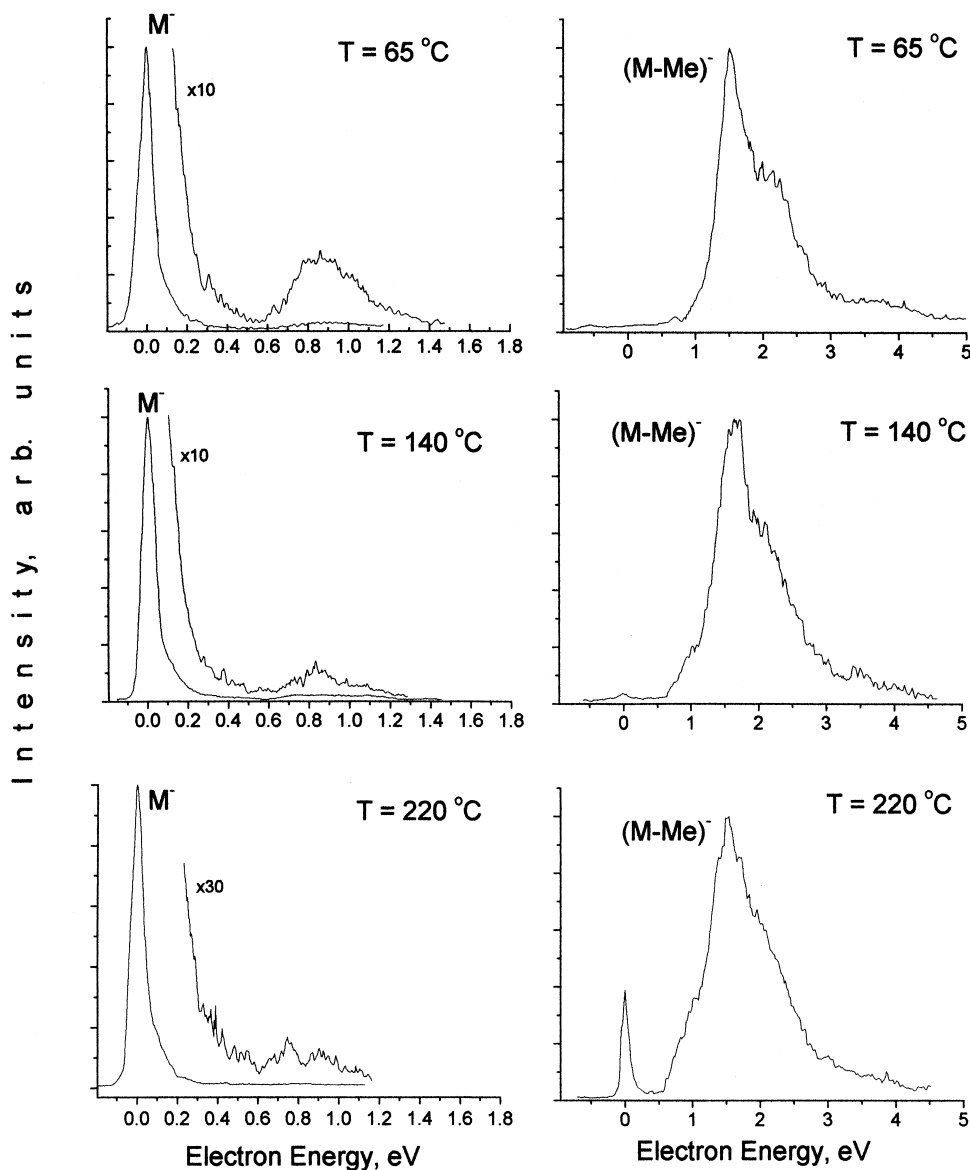
Fig. 12. Effective yield curves of the molecular M^- negative ions (left) and the fragment negative ions $H_3COC_6H_4N_2C_6H_4O^-$ (right; noted as $(M\text{-}Me)^-$ in the figure) from $p\text{-}OCH_3\text{-}p'\text{-}OCH_3\text{-}AzB$, plotted as a functions of the electron energy at the temperatures of 65°, 140°, and 220 °C.

taneous variation with temperature and the shape of the peaks remained constant. The finding is common for all the compounds studied. In contrast, other fragment ions behave differently with increasing temperature, and Figs. 12 and 13 indicate these observations in the case of $(M\text{-}Me)^-$ and NO_2^- from compounds 9 and 6, respectively.

Again, as in the case of *p*-nitrophenol 2, two additional resonant peaks at ~0 and 0.4 eV were observed for the $(M\text{-}H)^-$ ions when the temperature was raised. The intensity of the first signal at thermal energy for compounds 5 and 6 increased faster than the peak at 0.85 eV. For compound 7 both peaks were found to vary simultaneously with
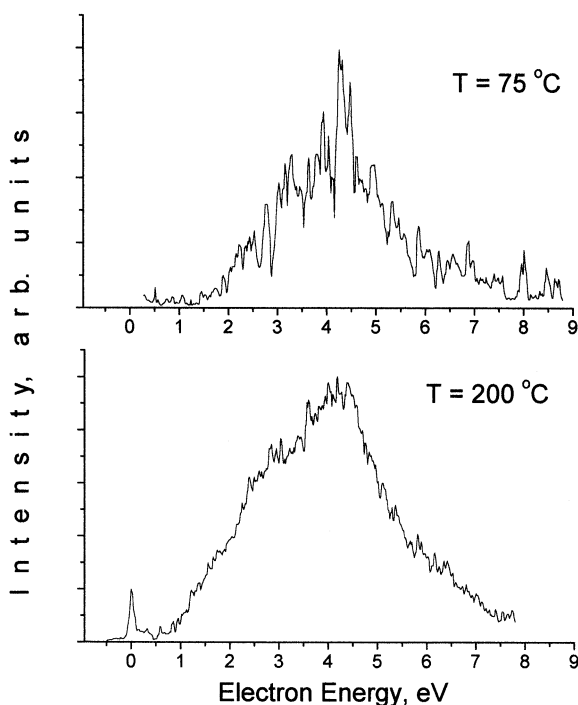
Fig. 13. Effective yield curves of the fragment negative ions from p-OH-p'-NO₂-AzB, plotted as a function of the electron energy recorded at the temperatures of 75° and 200 °C.

Fig. 14. Effective yield curve of the CF_3COO^- negative ions from CF_3COOH (TFA) plotted as a function of electron energy. Bars indicate the vibrational progression of the ν(OH) stretching mode.

temperature. For the second resonant peak at 0.4 eV on the yield curve of (M-H)⁻, we observed increasing intensity with increasing temperature for all compounds, and this with much larger rates than for the other resonant peaks at 0.85 eV and higher energies.

To determine the thermochemical threshold for the (M-H)⁻ formation from compound 5, we carried out semiempirical calculations of the enthalpies of formation of all involved species. This approach was chosen because of the lack of the necessary literature data. Based on these calculations and applying Eq. (1), the thermochemical limit for the (M-H)⁻ formation from compound 5 amounts to 0.68 eV (AM1) and to 0.60 eV (PM3). The match to the experimental value of 0.74 ± 0.05 eV is satisfactory. As a result, these data clearly show that the (M-H)⁻ ions from 5 at 0.4 eV and ~0 eV cannot by formed by OH bond cleavage.
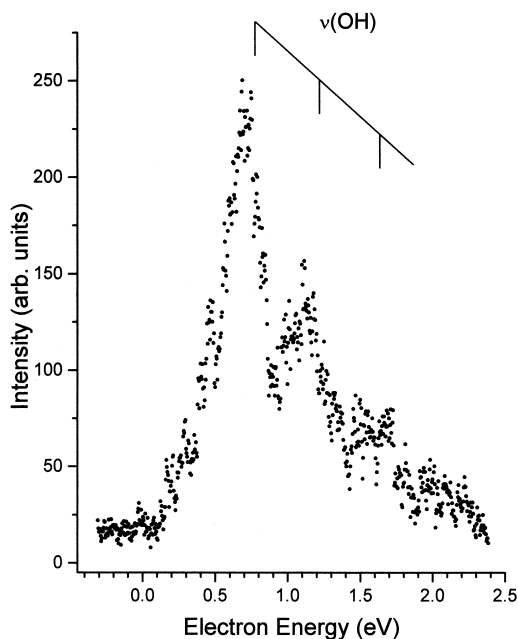
3.3. Trifluoroacetic acid (TFA)

The effective yield curves of (M-H)⁻ ions derived from compounds with TFA-related structures (acetic acid and acridanoneacetic acid) reveal an analogous vibrational fine structure [23,24]. To the best of our knowledge, the resonant electron capture spectra of TFA itself have not been reported in the literature and details will appear in a forthcoming paper. In the present article we restrict our considerations to the (M-H)⁻ formation from TFA. Fig. 14 shows the effective yield curve of (M-H)⁻ ions derived from TFA as a function of the energy in the range of ~0–2.5 eV. The yield curve is characterized by a prominent vibrational progression consisting of at least three overtones with a spacing of 0.43 eV between the peaks. Because there are no C-H bonds in this molecule the assignment of the high-frequency progression is unambiguous, namely, the excitation of the ν(OH) stretching mode.

4. Discussion

The vibrational progression observed in the effective yield curve of the (M-H)⁻ ions is in striking contrast to the assumption that their formation proceeds through a fast dissociation process. Such a scenario would result if the molecule could be directly driven into a purely repulsive electronic state of the anion following the electron capture event. The observed vibrational progression definitely indicates that at the formation energy of these negative ions an electronic state exists, which is stable for anions possessing the intact OH bond. Of particular importance is the assignment of the progression to the stretching mode of the OH bond, which eventually dissociates over time. The observation of the progression in the (M-H)⁻ effective yield curves of compounds 4 and 11, which possess only one H atom and only one high-frequency vibrational mode, confirms this assignment unambiguously.

The question arises as to whether or not these vibrations are excited immediately after electron attachment. According to the electron transmission spectrum of phenol [40], there exist two temporary anionic states in the energy range under discussion, namely, at 1.1 and 1.73 eV. The first of them is the $^2A_2$ ground state of the phenol anion and was observed in the transmission spectrum with a vibrational fine structure, showing an average spacing between the vibrational peaks of 120 meV. The second resonant state, $^2B_1$, was structureless, probably because of the shorter lifetime of the resonance. Based on the measurements of the appearance and peak energies of the (M-H)⁻ ions and the electron transmission spectrum [40], it is reasonable to assume that these fragment anions originate from the $^2A_2$ ground state of the phenol anion. Thus, these facts indicate that the ν(OH) stretch mode is not excited directly during the Franck-Condon transition from the ground state of the neutral molecule to the ground state of the molecular anion. Hence, it seems reasonable to assume that it is excited because a coupling with one or more other vibrational modes (possibly via Fermi resonances [41]) that are excited in the direct transition. Potential energy curves plotted in Fig. 15a illustrate this process schematically. Clearly, for the process to occur a finite period of time is required, and it is unclear at present whether or not other types of vibrations are also involved. We believe that the observation of the combined vibrational modes in the case of compound 5 (progression II on the curve of [M-H]⁻ in Fig. 5) gives a strong indication that this is really the case. We are not aware of electron transmission data for p-nitrophenol 2, but, on the basis of the experimentally determined energies of the resonant states from the dissociative electron capture spectra of related nitrobenzenes [27] and considering the present findings on the resonant electron capture processes of hydroxy azobenzenes, we can deduce that the (M-H)⁻ ions from 2 at ~0.65 eV are also formed from the ground state of the anion.

The situation in hydroxy azobenzenes is different in that these molecules form long-lived molecular negative ions over a wider electron energy range, that is, from ~0 to 1–1.5 eV. In compound 6, for example, it was possible to register both parent and fragment (M-H)⁻ ions in the energy range of 0.5–1.6 eV. As mentioned above, the ν(OH) overtone progression commences in the curve of molecular ions, M⁻ (point C in Fig. 15b). This finding definitely shows that the dissociation under discussion again occurs via the ground state of the molecular negative ion. There is no dissociation at the first peak of the progression because the energy of the resonant peak is lower than the thermochemical dissociation limit. Thus, excitation of these vibrational modes does not always lead to dissociation, and the need to explain why excitation of these vibrational modes may also result in long-lived molecular ions becomes obvious.

For AzBs one can expect several unoccupied π^* orbitals with positive energies relative to the molecular ground state. The capture of the incoming electrons into these orbitals might result in π^*-shape resonances as found in analogy for the π-isoelectronic stilbene molecule [30]. Furthermore, in AzBs there exist also low-lying n-π^* and π-π^* triplet states with transition energies of 1.52 and 1.9–2.1 eV, respectively [42,43]. Thus, long-lived molecular negative ions of AzBs in the vicinity of 1 eV might be formed via electron-excited Feshbach resonances, the parent
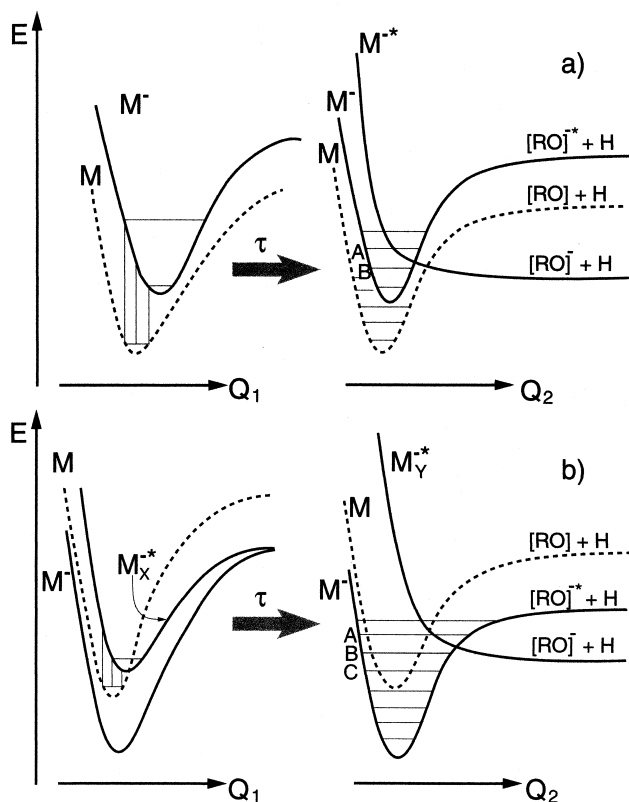
Fig. 15. Schematic potential energy curves illustrating the formation of (M-H)$^-$ ions by O-H bond cleavage via predissociation for (a) phenol and (b) oxy azobenzene. Q_1 and Q_2 represent different motions in a negative ion.

states of which would represent just these triplet states, possibly even singlet-excited states with the same symmetry. In fact, increasing the abundance of the long-lived molecular ions of 7 by increasing the temperature in the energy range of 0.9–1.4 eV can be regarded as a similar process to the known phenomenon of increasing the intensity of the n-π^* singlet transition with elevated temperatures [44]. An energy of 0.4 eV is, however, too low to assign the resonant peak at this energy to these Feshbach resonances. Therefore, it is more probable to assume a shape-resonance mechanism by electron capture into one of the π^* orbitals. While initially formed via different mechanisms, all these parent anions observable by mass spectrometry are converted through radiationless transitions into different vibrational levels of the anionic ground state before their detection. According to theoretical considerations on nonradiative transi-

tions [45], internal conversion between two electronic states that are separated by a large enough gap occurs more efficiently if high-frequency vibrations are involved. In this respect, excitation of the ν(OH) mode in an anionic excited state resulting in conversion into the ground state is not surprising. Excitation of the next vibrational overtone (again via Fermi resonance) leads to dissociation of the OH bond with formation of (M-H)$^-$ ions. However, the simultaneous observation of parent and fragment anions, as in the case of compound 6, gives an obvious indication that the ground state of the parent negative ion may be stable with respect to the OH bond cleavage even at energies equal to or higher than the dissociation threshold (see Fig. 15). Considering the symmetry of the anionic ground state, there might exist an analogy to chlorobenzene [18] in that the dissociation asymptote of the ground state is probably slightly exceeding the ther-

mochemical threshold of 1.29 eV in 5 (or 1.497 eV according to Eq. (1)). This would correspond to the separated species of H-atom and the electronically excited state of $(M\text{-}H)^{-*}$ being of the same symmetry as the anionic ground state. Therefore, one may conjecture that the formation of $(M\text{-}H)^{-}$ in hydroxy azobenzenes proceeds by predissociation from the ground anionic state, bonding along the OH bond at these energies (point B in Fig. 15), into another electronic state with the repulsive along the OH bond surface by a tunneling mechanism. Predissociation from the next excited vibrational level (point A in Fig. 15) occurs probably over a barrier, but because of unfavourable interaction of the two states at this level (small Franck-Condon factors), the ion intensity will hardly be higher than in the previous case. The ratio of the ion yields derived from these two vibronic states (see previous section) will probably depend on the position of the intersection of the anion's ground and excited states regarding the vibrational level indicated as point A in Fig. 15.

Two experimental findings are in strong support of the tunneling character of the dissociation at threshold. First, the shape of the effective yield curve of $(M\text{-}H)^{-}$ ions is temperature independent over the entire energy range in which vibrational progression $\nu(OH)$ is observed. Second, the experimental appearance energies alongside the peak energies for $(M\text{-}Me)^{-}$ ions derived from OMe group–containing precursor 8 and 10 always show larger values than those obtained for the $(M\text{-}H)^{-}$ ions under discussion. This seems surprising on first sight, considering the well-known fact that the bond dissociation energy of the O-Me bond is lower than that of OH. For example, the O-Me bond in anisole is 22.7 kcal mol^{-1} less stable than the O-H bond in phenol [33]. Peak energy for the formation of $(C_6F_5O)^{-}$ ions from pentafluorophenol was also found to be lower than in the case of pentafluoroanisole [27]. The present observation may be caused by the higher mass of the Me-group, which should lead to a dramatically decreased dissociation probability if tunneling played a major mechanistic role. As a consequence, the $(M\text{-}Me)^{-}$ anions are always observed at higher energies, probably located in the vicinity of the top of the dissociation barrier/

asymptote. Contrary to the behavior of the $(M\text{-}H)^{-}$ ions, the shape of the $(M\text{-}Me)^{-}$ effective yield curve changes with temperature leading to a broadening of the curve accompanied by a gradual lowering of the appearance energy (Fig. 12). These features are clear indications of a classical behavior of this type of dissociation reaction. Indeed, in the temperature range applied here, only low-frequency vibrations may be excited efficiently, and the resonance couplings of these vibrations with the reaction coordinate might result in a smooth reduction of the appearance energy. A similar behavior was observed for NO_2^{-} ions from 6 and 9 (see Fig. 13 for compound 6).

The resonant peak observed at lower energies than the main peak of $(M\text{-}H)^{-}$, which is spaced by a magnitude of the vibrational quanta $\nu(OH)$, deserves further consideration. The intensity of this resonant peak increases with elevated temperatures relative to the main peak for all compounds for which the electron capture was studied as a function of the temperature. Because the energy of this resonance is lower than the thermochemical threshold, we connect this resonant peak with a transition from the thermally excited level of the $\nu(OH)$ vibrational mode. The main problem with this suggestion is the low number of thermally excited species owing to the very large magnitude of the vibrational quanta. At a temperature of 520 K the ratio of these molecules is only ca. 4×10^{-5} relative to the total number of molecules. However, the experimental data undoubtedly emphasize the key role of the $\nu(OH)$ stretching mode. Therefore, we suggest that the rate-determining step of the reaction is, in fact, the excitation of the $\nu(OH)$ stretching mode, which involves energy exchange between vibrational modes before the internal energy is concentrated in this mode. This process is supposed to take a long period of time. The preceding thermal excitation of this mode in the neutral can reduce the required time to a great extent. In contrast, electron autodetachment in the parent negative ion may play a dramatic role when a significant part of these species undergo the autodetachment process before the dissociation reaction, where the $\nu(OH)$ stretching mode was not excited beforehand. This would lead to a situation in which both the relative intensity of the
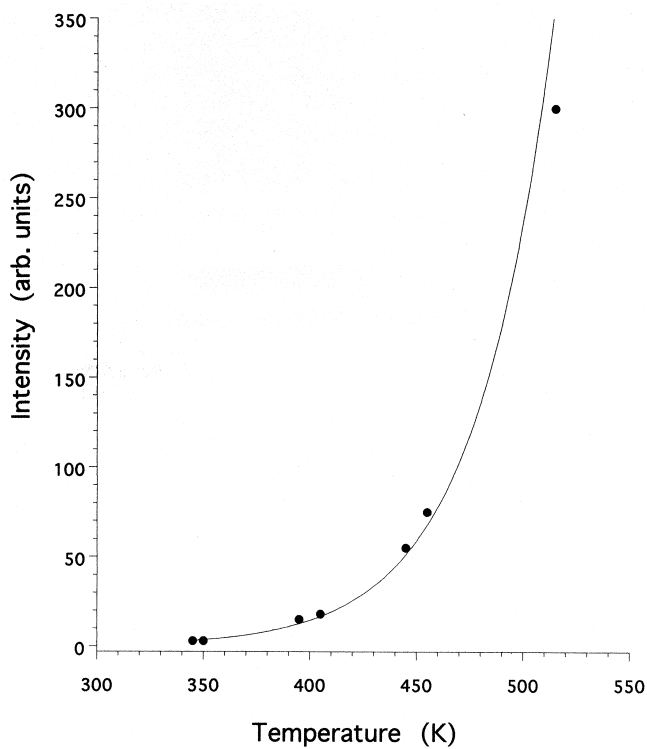
Fig. 16. Dependence of the yield of (M-H)⁻ fragment negative ions from *p*-OH-AzB at the resonant peak 0.4 eV plotted as a function of the temperature (circles) and population of the vibrational level of the ν(OH) stretching mode with temperature (line).

"normal" resonant peak of (M-H)⁻ ions and the one associated with the transition from the "hot band" became comparable at higher temperatures. To confirm these thoughts, Fig. 16 provides a comparison of the intensity of (M-H)⁻ ions from 5 at the resonant energy of 0.4 eV as a function of the temperature and the calculated normal Boltzmann distribution. The latter indicates the increase of the population of the excited vibrational level (ν(OH) mode) at elevated temperatures. Both the curves were normalized to each other at a middle temperature point of 405 K. As can be seen at least for the explored temperature range, the agreement between the two curves is quite good.

The origin of the resonant peak of (M-H)⁻ ions at thermal energies is unclear. Again, its maximum is much lower than the thermochemical threshold. As mentioned above, different compounds showed different intensities. One plausible explanation in the case of hydroxy azobenzenes might be associated with the presence of different isomers. The trans- and cis-isomers of azobenzenes [44] should show a similar behavior under the present conditions. The common azo form can, however, also exist as a tautomeric hydrazone form [44], for which the initial OH hydrogen is located at the azo group and the phenyl ring appears as a quinonic structure. As to whether or not this tautomer is of importance here cannot be answered by the present experiments. The enthalpies of formation for the different isomeric forms of azobenzenes were calculated earlier on the basis of the isodesmic reactions [21], including isomers with H-attachment to the azo group. It was shown that such isomeric forms should be characterized by a low value of the BDE. It is also possible that related rearrangement processes, leading to configurations with the H-atom on the azo group, may occur in the anions that are formed at thermal energies. Analogous processes

may take place in nitrophenols, where (M-H)$^-$ ions were also observed at energies near 0 eV. It is obvious that more comprehensive investigations into this matter are needed to provide a more definite answer.

5. Conclusion

Several OH group–containing benzene and azobenzene derivatives have been studied by negative-ion mass spectrometry in the resonant electron capture mode. Special emphasis has been paid to the low-energy formation of (M-H)$^-$ fragment ions. It has been established that these ions are formed practically at the thermochemical threshold of the OH bond cleavage in the anion. The process was found to be independent of the molecular symmetry and the symmetry of the parent resonant state. The ion yield curves for all these ions show a vibrational fine structure in an energy range near the threshold of formation. The analysis of this structure was carried out for all these molecules on the basis of known vibrational frequencies, and it was possible to assign this vibrational progression to the excitation of the ν(OH) stretching mode. It has been possible to deduce that the formation of these ions at the threshold is not a direct dissociation process but very likely the result of predissociation through a tunneling mechanism. The use of higher electron-energy resolution than applied in the given work would be helpful to obtain further insight into this phenomenon. In particular, this would be of interest for the case of oxy azobenzenes, as the mean lifetime of the molecular negative ions is long enough and assignment of the combined vibrational modes together with the discussed ν(OH) stretching mode would allow more detailed elucidation of the predissociation mechanism.

References

[1] J.C. Lorquet, Org. Mass Spectrom. 16 (1981) 469.
[2] J.C. Lorquet, Mass Spectrom. Rev. 13 (1994) 233.
[3] T. Sewell, D.L. Thompson, R.D. Levine, J. Phys. Chem. 96 (1992) 8006.
[4] C.E. Klots, J. Chem. Phys. 46 (1967) 1197.
[5] C. Lifshitz, Mass Spectrom. Rev. 12 (1993) 261.
[6] P. Wurz, K.R. Lykke, J. Phys. Chem. 96 (1992) 10129.
[7] C. Yeretzian, K. Hansen, R.L. Whetten, Science 260 (1993) 652.
[8] T. Jaffke, E. Illenberger, M. Lezius, S. Matejcik, D. Smith, T. Märk, Chem. Phys. Lett. 226 (1994) 213.
[9] O. Elhamidi, J. Pommier, R. Abouaf, J. Phys. B At. Mol. Opt. Phys. 30 (1997) 4633.
[10] A. Bekkerman, B. Tsipinyuk, E. Kolodney, Int. J. Mass Spectrom. 185/186/187 (1999) 773.
[11] Yu.V. Vasil'ev, R.F. Tuktarov, V.A. Mazunov, Rapid Commun. Mass Spectrom. 11 (1997) 757.
[12] H.S. Massey, Negative Ions, Cambridge University Press, Cambridge, 1976.
[13] S.F. Wang, G.J. Shulz, Phys. Rev. Lett. 35 (1975) 1429.
[14] G.A. Gallup, Phys. Rev. A. 34 (1986) 2746.
[15] G.A. Natanson, J. Phys. B At. Mol. Phys. 18 (1985) 4481.
[16] J. Simons, J. Am. Chem. Soc. 103 (1981) 3971.
[17] V.I. Khvostenko, R.S. Rafikov, Dokl. Akad. Nauk SSSR, 220 (1975) 892 (in Russian).
[18] D.D. Clarke, C.A. Coulson, J. Chem. Soc. (A)1 (1969) 169.
[19] L.G. Christophorou, Atomic and Molecular Radiation Physics, Willey Interscience, London, NY, 1971.
[20] K.L. Stricklett, P.D. Burrow, J. Phys. B Atom. Mol. Phys. 19 (1986) 4241.
[21] M.V. Muftakhov, Yu.V. Vasil'ev, V.A. Mazunov, V.V. Takhistov, D.A. Ponomarev, J. Mass Spectrom. 30 (1995) 257.
[22] Yu.V. Vasil'ev, V.A. Mazunov, Fizika v Bashkortostane (Physics in Bashkortostan), in: A.M. Prokhorov (Ed.), Ufa, Hilem, pp. 78–101 (in Russian).
[23] M.V. Muftakhov, Yu.V. Vasil'ev, V.A. Mazunov, Rapid Commun. Mass Spectrom. 13 (1999) 1104.
[24] M.V. Muftakhov, Yu.V. Vasil'ev, R.V. Khatymov, V.A. Mazunov, V.V. Takhistov, O.V. Travkin, E.V. Yakovleva, Rapid Commun. Mass Spectrom. 13 (1999) 912.
[25] N.L. Asfandiarov, V.S. Fal'ko, A.I. Fokin, G.S. Lomakin, N.M. Pozdeev, O.Yu. Podkopaeva, Yu. V. Chizov, Rapid Commun. Mass Spectrom. 12 (1998) 595.
[26] N.L. Asfandiarov, A.I. Fokin, V.G. Lukin, E.P. Nafikova, G.S. Lomakin, V.S. Fal'ko, Yu.V. Chizov, Rapid Commun. Mass Spectrom. 13 (1999) 1116.
[27] W.T. Naff, R.N. Compton, C.D. Cooper, J. Chem. Phys. 54 (1971) 212.

[28] L.G. Christophorou, Adv. Electron. Electron Phys. 46 (1978) 55.

[29] O. Ingolfson, F. Weik, E. Illenberger, Int. J. Mass Spectrom. Ion Processes 155 (1996) 1.

[30] K.D. Jordan, P.D. Burrow, Chem. Rev. 87 (1987) 557.

[31] M. Allan, J. Electron Spectrosc. Relat. Phenom. 48 (1989) 219.

[32] D.R. Lide (Ed.), CRC Handbook of Chemistry and Physics, CRC, Boca Raton, FL, 1991.

[33] D.F. McMillen, D.M. Golden, Ann. Rev. Phys. Chem. 33 (1982) 493.

[34] V.V. Takhistov, M.V. Muftakhov, A.A. Krivoruchko, V.A. Mazunov, Izvestija AN SSSR, ser. Khim. (Sov. Chem. Bull.), 9 (1991) 2049 (in Russian).

[35] Yu.V. Vasil'ev, V.A. Mazunov, JETP Lett. 51 (1990) 145.

[36] Yu.V. Vasil'ev, V.A. Mazunov, Dokl. Akad. Nauk SSSR (Sov. Phys. Doklady), 315 (1990) 637 (in Russian).

[37] Yu.V. Vasil'ev, V.A. Mazunov, Khimicheskaya Fizika (Sov. Chem. Phys. Reports), 10 (1990) 170 (in Russian).

[38] Yu.V. Vasil'ev, V.A. Mazunov, E.R. Nazirov, Org. Mass Spectrom. 26 (1991) 739.

[39] D.R. Armstrong, J. Clarkson, W.E. Smith, J. Phys. Chem. 99 (1995) 17825.

[40] K.D. Jordan, J.A. Michejda, P.D. Burrow, J. Am. Chem. Soc. 98 (1976) 7189.

[41] G. Herzberg, Molecular Spectra and Molecular Structure. Vol. 3. Electronic spectra and Electronic Structure of Polyatomic Molecules. Van Nostrand, Princeton, NJ, 1966.

[42] S. Monti, E. Gardini, P. Bortolus, E. Amonyal, Chem. Phys. Lett. 77 (1981) 115.

[43] S. Monti, S. Dellone, P. Bortolus, J. Photochem. 23 (1983) 249.

[44] H. Rau, Angew. Chem. Int. Edit. Engl. 12 (1973) 224.

[45] P. Avorius, W.M. Gelbart, M.A. El-Sayed, Chem. Rev. 77 (1977) 793.